EBioMedicine 20 (2017) 109–119

Contents lists available at ScienceDirect

EBioMedicine

journal homepage: www.ebiomedicine.com

Research Paper

The Transcriptional Landscape of p53 Signalling Pathway

Chizu Tanikawa [a], Yao-zhong Zhang [b], Ryuta Yamamoto [a], Yusuke Tsuda [a], Masami Tanaka [a], Yuki Funauchi [a], Jinichi Mori [a,c], Seiya Imoto [b], Rui Yamaguchi [b], Yusuke Nakamura [d,f], Satoru Miyano [b], Hidewaki Nakagawa [e], Koichi Matsuda [a,c,*]

[a] Laboratory of Molecular Medicine, Human Genome Center, Institute of Medical Science, University of Tokyo, Tokyo, Japan
[b] Laboratory of DNA information Analysis, Human Genome Center, Institute of Medical Science, University of Tokyo, Tokyo, Japan
[c] Laboratory of Clinical Genome Sequence, Department of Computational Biology and Medical Sciences, Graduate School of Frontier Sciences, University of Tokyo, Tokyo, Japan
[d] Department of Medicine, Center for Personalized Therapeutics, The University of Chicago, USA
[e] Laboratory for Genome Sequencing Analysis, RIKEN Center for Integrative Medical Sciences, Tokyo, Japan
[f] Department of Surgery, Center for Personalized Therapeutics, The University of Chicago, USA

ARTICLE INFO

Article history:
Received 3 March 2017
Received in revised form 9 May 2017
Accepted 10 May 2017
Available online 18 May 2017

Keywords:
p53
Transcriptome
Radiation
Keratinization

ABSTRACT

Although recent cancer genomics studies have identified a large number of genes that were mutated in human cancers, *p53* remains as the most frequently mutated gene. To further elucidate the p53-signalling network, we performed transcriptome analysis on 24 tissues in $p53^{+/+}$ or $p53^{-/-}$ mice after whole-body X-ray irradiation. Here we found transactivation of a total of 3551 genes in one or more of the 24 tissues only in $p53^{+/+}$ mice, while 2576 genes were downregulated. *p53* mRNA expression level in each tissue was significantly associated with the number of genes upregulated by irradiation. Annotation using TCGA (The Cancer Genome Atlas) database revealed that p53 negatively regulated mRNA expression of several cancer therapeutic targets or pathways such as *BTK*, *SYK*, and *CTLA4* in breast cancer tissues. In addition, stomach exhibited the induction of Krt6, Krt16, and Krt17 as well as loricrin, an epidermal differentiation marker, after the X-ray irradiation only in $p53^{+/+}$ mice, implying a mechanism to protect damaged tissues by rapid induction of differentiation. Our comprehensive transcriptome analysis elucidated tissue specific roles of p53 and its signalling networks in DNA-damage response that will enhance our understanding of cancer biology.

1. Introduction

Although recent cancer genome analysis has uncovered a large number of genes that are mutated in various cancer types, *p53* remains the most frequently mutated gene in cancer cells. Somatic mutations of *p53* are more frequent in ovarian (Patch et al., 2015) and esophageal (Dulak et al., 2013) cancers, and osteosarcoma (Chen et al., 2014) (>50%) but relatively rare in leukaemia, neuroblastoma, and thyroid carcinoma (Cancer Genome Atlas Research, 2013, 2014b; Ramsay et al., 2013) (<10%), indicating a diverse mutation spectrum for the *p53* gene across tissues. Inherited mutations in *p53* also cause an early-onset familial cancer syndrome, in which glioblastoma, osteosarcoma, and leukaemia are frequently observed (Malkin et al., 1990). Moreover, non-synonymous single nucleotide polymorphisms (SNPs) or rare variations in the *p53* gene are associated with an increased susceptibility to cancer and poor prognosis (Shiraishi et al., 2010; Stacey et al., 2011). Mouse models have also revealed important roles for p53; >70% of $p53^{-/-}$ mice are prone to the spontaneous development of a neoplasm by 6 months of age (Donehower et al., 1992; Jacks et al., 1994). Most of the tumors in $p53^{-/-}$ mice are lymphomas (71%), while sarcoma (57%) occurs more frequently than lymphomas (25%) in $p53^{+/-}$ mice (Jacks et al., 1994). Furthermore, tissue-specific inactivation of p53 accompanied with (or without) other genetic alterations results in the development of mammary carcinomas, oral-oesophageal cancer, pancreatic ductal cancer, or liver cancer (Cao et al., 2003; Hingorani et al., 2005; Liu et al., 2007; Opitz et al., 2002; Xue et al., 2014).

Genotoxic stresses, such as DNA damage, oxidative stress, and hypoxia, induce phosphorylation and stabilization of the p53 protein (Vogelstein et al., 2000). Activated p53 functions as a transcription factor and suppresses cell growth *via* transactivation of its target genes involved in apoptosis, cell cycle arrest, and/or senescence (Nakamura, 2004; Vogelstein et al., 2000). Additionally, p53 regulates various biological processes, such as metabolic pathways, aging, development,

Abbreviations: TCGA, The Cancer Genome Atlas; FPKM, fragments per kilobase of transcript per million mapped reads; qPCR, quantitative Polymerase Chain Reaction; GO, Gene ontology; K, $p53^{-/-}$ mice without irradiation; W, $p53^{+/+}$ mice without irradiation; KX, $p53^{-/-}$ mice with X-ray irradiation; WX, $p53^{+/+}$ mice with X-ray irradiation.

* Corresponding author at: Laboratory of Clinical Genome Sequencing, Department of Computational Biology and Medical Sciences, Graduate School of Frontier Sciences, University of Tokyo, 4-6-1 Shirokanedai, Minato, Tokyo 108-8639, Japan.
E-mail address: kmatsuda@k.u-tokyo.ac.jp (K. Matsuda).

http://dx.doi.org/10.1016/j.ebiom.2017.05.017

reprogramming, and reproduction (Hu et al., 2007; Kang et al., 2009; Kruiswijk et al., 2015). Thus, p53 exhibits various physiological functions in a context-dependent and tissue-specific manner.

Previous studies have identified a number of p53 target molecules using transcriptome analysis of specific cell lines, tissues, or mouse embryonic fibroblasts (MEFs) (Kenzelmann Broz et al., 2013; Masuda et al., 2006) (Table S1). However, no systematic analysis of p53 target genes in various tissues has been conducted thus far. To elucidate the role of p53 at individual tissue levels, we performed whole-body transcriptome analysis after X-ray-irradiation on $p53^{+/+}$ and $p53^{-/-}$ mice. In our study, 280 samples from 24 tissues were evaluated by RNA sequence analysis. Our study is the comprehensive analysis of the p53 signalling pathway *in vivo*.

2. Materials and Methods

2.1. Mice and X-ray Treatment

$p53^{-/-}$ mice were provided from the RIKEN BioResource Center (Ibaragi, Japan) (Tsukada et al., 1993). 5′ part of exon 2 including translation initiation site was replaced with Neomycin resistance gene (Neor). Genotypes were confirmed by PCR analysis. The primer sequences are presented in Table S2.

All mice were maintained under specific pathogen-free conditions and were handled in accordance with the Guidelines for Animal Experiments of the Institute of Medical Science (University of Tokyo, Tokyo, Japan). $p53^{+/+}$ and $p53^{-/-}$ mice were X-ray-irradiated using the MBR-1520R-3 system (Hitachi, Tokyo, Japan). At 24 h after irradiation, 24 tissues were collected from mice. The age and gender of mice are shown in Fig. 1A. Tissues were preserved in RNAlater solution (QIAGEN) at 4 °C until RNA purification. Bone marrow was resolved in RLT plus reagent provided by the RNeasy Plus Mini Kit (QIAGEN) and homogenized using a QIAshredder column (QIAGEN). The lysates were stored at −80 °C until RNA purification.

2.2. RNA Sequencing

Tissues were homogenized in QIAzol lysis reagent (QIAGEN) using Precellys 24 (Bertin Corporation). Total RNA was recovered using the RNeasy Plus Universal Mini Kit (QIAGEN). For RNA extraction from bone marrow, we used the RNeasy Plus Mini Kit (QIAGEN). We selected 280 samples for RNA sequencing analysis based on RNA quality and quantity, which were evaluated using a Bioanalyzer (Agilent) and Nanodrop (Thermo Fisher Scientific). High-quality RNA was subjected to polyA+ selection and chemical fragmentation, and a 100–200 base RNA fraction was used to construct complementary DNA libraries

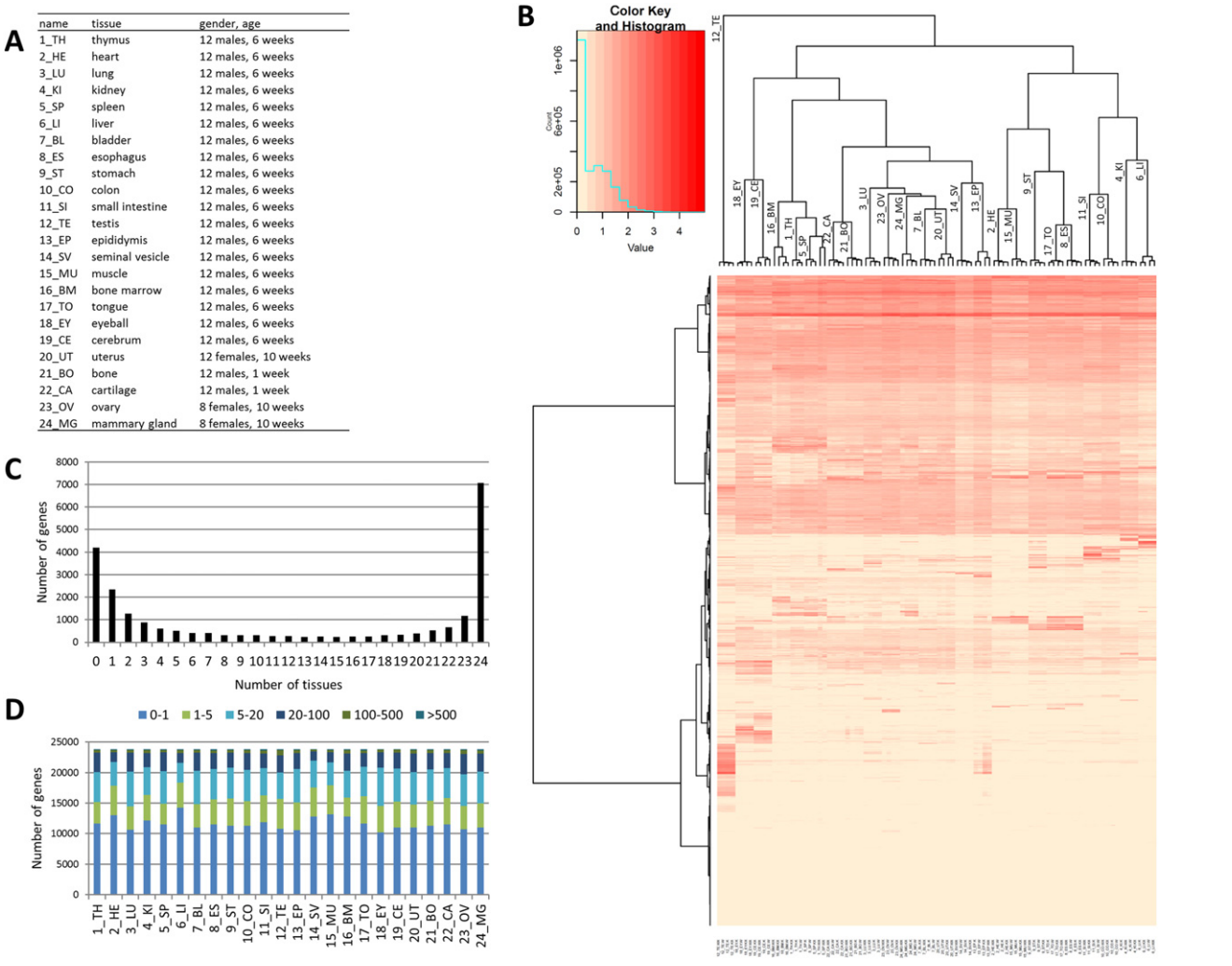

Fig. 1. Whole-body transcriptome analysis of $p53^{+/+}$ and $p53^{-/-}$ mice. A, List of 24 tissues used in this analysis. Age, gender, and number of mice are shown. B, The dendrogram derived from a cluster analysis using expression levels of 23,813 transcripts in 96 groups (K, W, KX, and WX, 24 tissues each) is shown with heatmap. We calculated the mean FPKM value for all samples from each tissue condition and performed a log(FPKM + 1) transformation before clustering. Clustering distance was based on "Euclidean" distance. C, Genes were categorized based on the number of expressed tissues (FPKM > 1) in wild-type mice. The average FPKM values for each gene and tissue were used in the analysis. D, Genes were categorized based on their expression level in wild-type mice. The average FPKM values for each gene and tissue were used in the analysis.

according to Illumina's protocol. RNA-seq was performed on a HiSeq 2500 using a standard paired-end 101-bp protocol. The raw data obtained in this study can be accessible in DDBJ database (http://www.ddbj.nig.ac.jp/index-e.html) with accession number of DRA005768 with bioproject accession number of PRJDB5738.

2.3. Quantitative Real-time PCR

Complementary DNAs were synthesized with the SuperScript Preamplification System (Invitrogen). Quantitative real-time PCR was conducted using the SYBR Green I Master Mix on a LightCycler 480 (Roche). The primer sequences are shown in Table S2.

2.4. Data Analysis of RNA Sequencing

We used a tophat + cufflinks pipeline to process raw RNA-seq data. Before data processing, the quality of data was checked with FastQC. To quantify gene and transcript expression levels for all samples, we first aligned 101 bp paired-end reads to the mouse reference genome mm9/GRCm37 using Tophat (v2.0.9). The mapping parameters follow the default setting in the Tophat. After the read mapping, transcript and gene expression levels, which are represented by FPKM (fragments per kilobase of transcript per million mapped reads) values, were calculated by Cufflinks (v2.2.1). We used the transcript/gene abundant as a sample profiler for the downstream bioinformatics analysis.

2.5. Other Bioinformatics Analysis

KEGG pathway analyses and GO term analyses were performed using DAVID (https://david.ncifcrf.gov/). Relative scores were calculated as follows: -log10(*P* value) × log2(Fold enrichment). GO reduction and connectivity graphs were generated using REVIGO (http://revigo.irb.hr/) and Cytoscape version 3.2.1 (http://www.cytoscape.org/). For clustering, the mean FPKM value for all samples of each tissue condition was calculated, and a log (FPKM + 1) value was used. Clustering analysis was conducted using the R program based on "Euclidean" distance. We used the Basic R program to generate correlation plots.

2.6. TCGA (The Cancer Genome Atlas) Data

Gene expression data and *p53* mutation status in clinical samples were obtained from the TCGA data portal (https://tcga-data.nci.nih.gov/tcga/).

2.7. Gene Reporter Assay

The potential p53 binding sites around Krt5, Krt6a, Krt6b, Krt14, Krt16, and Krt17 were subcloned into the pGL4.24 vector (Promega). The 30 candidate sites are shown in Table S3. Oligonucleotides are presented in Table S2. Reporter assays were performed using the Dual Luciferase assay system (Promega) as previously described (Mori et al., 2016).

2.8. Immunohistochemistry

The formalin-fixed, paraffin-embedded mouse tissue sections were used for immunohistochemistry. Immunohistochemistry was performed using the immunohistochemistry EnVision (Dako) method. The antibodies and the concentrations used are shown in Table S4.

2.9. Western Blotting

To prepare whole-cell extracts, tissues were homogenized in chilled RIPA buffer using Precellys 24 (Bertin Corporation) and centrifuged at 16,000*g* for 15 min. Samples were subjected to SDS–PAGE and immunoblotting using standard procedures. The antibodies and the concentrations used are shown in Table S4.

3. Results

3.1. RNA Sequence Analysis

To determine the appropriate dosage of X-ray in our screening, I evaluatd mRNA expression of four p53 targets (*Cdkn1a*, *Fas*, *Mdms*, and *Bax*) in three representative tissues (thymus, spleen, and liver) from $p53^{+/+}$ mice those were exposed with 2, 5, or 10 Gy of X-ray (n = 3 each). The result of qPCR (quantitative Polymerase Chain Reaction) analysis indicated that all four p53-targets showed dose-dependent induction in liver (Fig. S1A). In contrast, *Bax* expression level was similar among 2, 5, and 10 Gy in thymus and spleen. These results indicated substantial difference in X-ray sensitivity among tissues and genes. In this study, we selected 10 Gy of X-ray to increase possibility to identify p53-targets even in X-ray resistant tissues.

To fully understand transcriptional regulation of p53-downstream genes in response to DNA damage, we irradiated both $p53^{+/+}$ and $p53^{-/-}$ mice with 10 Gy of X-ray and then isolated RNAs from 280 samples derived from 24 tissues (Fig. 1A and Table S5). Samples we analyzed were categorized into 4 groups: (K) $p53^{-/-}$ mice without irradiation, (W) $p53^{+/+}$ mice without irradiation, (KX) $p53^{-/-}$ mice with X-ray irradiation, and (WX) $p53^{+/+}$ mice with X-ray irradiation. qPCR analysis of known p53 targets, *Cdkn1a*/*p21*, *Mdm2*, *Bax*, and *Fas* indicated activation of p53 in response to X-ray irradiation in most of tissues in the WX group (Fig. S1B). On the other hand, p53 protein was increased by X-ray irradiation only in nine tissues (lung, bladder, esophagus, stomach, epididymis, seminal vesicle, uterus, ovary, and mammary gland) among 22 tissues analyzed (Fig. S2). Due to difficulty in protein extraction, we excluded bone and cartilage from this analysis. Thymus, heart, kidney, spleen, liver, testis, and tongue showed high basal p53 expression and no/marginal induction by X-ray, while colon, small intestine, muscle, bone marrow, eye, and cerebrum shows low expression even after X-ray irradiation, although Cdkn1a was induced in the most of tissues. In response to DNA damage, p53 is considered to be phosphorylated and stabilized, resulting in accumulation of protein that then activates its downstream targets (Vogelstein et al., 2000). However, our results revealed large diversity in the mechanism of p53 activation among tissues.

Subsequently, we quantified expression levels of 23,813 transcripts and 30,563 isoforms in a total of 280 samples from 24 different tissues as FPKMvalues (Table S6 and S7). We also confirmed clear correlation between qPCR results and RNA sequence data for *Cdkn1a*/*p21*, Mdm2, Bax, and Fas (Fig. S1B, C). We also confirmed the replacement of 5′ part of exon 2 including translation initiation codon of the *p53* gene by reads mapping, although p53 expression was not affected by X-ray (Fig. S3A—C). Through a cluster analysis of RNA sequence data (96 groups from 24 tissues), RNAs from spleen and thymus of WX mice were clustered into the same group (Fig. 1B and S4), in concordance with the high radiosensitivities of these two tissues (Komarova et al., 1997; Lowe et al., 1993).

We found that 19,609 genes were expressed (>1 of FPKM) in at least one tissue (Fig. 1C, D). Previous multi-tissue omics analyses used the threshold of 1 (FPKM value) for detectable gene (Uhlen et al., 2015). To exclude genes with very low expression, we used stringent filtering criteria for calculation of fold change by adding one to each FPKM value as reported previously (Brooks et al., 2011; Kaartokallio et al., 2015). >50 genes were significantly decreased in the uterus and brain of $p53^{-/-}$ mice compared with those in $p53^{+/+}$ mice (Fig. S5A). Gene ontology (GO) analysis indicated that the genes involved in gamma-aminobutyric acid signalling pathway and cholesterol biosynthetic process were downregulated in the brain and uterus of $p53^{-/-}$ mice,

respectively (Table S8 and Fig. S5B), suggesting possible roles of p53 in neurotransmission and cholesterol biosynthesis.

3.2. Role of p53 in the DNA Damage Response

We calculated the number of genes whose expression were induced or repressed more than twofold after X-ray irradiation in either $p53^{+/+}$ or $p53^{-/-}$ mice. We defined these genes as "X-ray-responsive genes". We found a significant diversity in the X-ray response among individual tissues, as 22.5% of genes (5352 of 23,813 genes) were altered after X-ray irradiation in the thymus, but <0.2% (51 of 23,813 genes) were altered in testis (Fig. 2A). Among the 5352 X-ray-responsive genes in thymus, most genes were induced or repressed only in $p53^{+/+}$ mice but not in $p53^{-/-}$ mice (Fig. S6). Based on the relative changes after X-ray irradiation in $p53^{+/+}$ or $p53^{-/-}$ mice, X-ray-responsive genes were categorized into 8 groups (Fig. 2B). Most of X-ray-responsive genes were induced or repressed only in $p53^{+/+}$ mice in all of the 24 tissues except eye, cerebrum, and epididymis. In eye and cerebrum, the majority of X-ray responsible genes were induced or repressed only in $p53^{-/-}$ mice, while response to X-ray in epididymis tissues was similar between $p53^{+/+}$ and $p53^{-/-}$ mice. When the induction/repression pattern was not identical between $p53^{+/+}$ and $p53^{-/-}$ mice, we defined those as p53-dependent X-ray responsive genes. Genes induced or repressed only in p53 knockout mice, p53 might have function to maintain sustainable gene expression. In summary, X-ray irradiation affected mRNA expression of the great majority (>80%) of X-ray responsible genes only in $p53^{+/+}$ mice or only in $p53^{-/-}$ mice (Fig. 2C), suggesting p53 as a key regulator in the DNA damage response.

3.3. Screening of p53 Targets

We screened p53-induced and p53-repressed genes that are significantly increased or decreased more than twofold in WX mice compared with other groups (Fig. 3). As shown in Fig. 4A, 3,069 and 1467 genes were significantly induced in the thymus and spleen uniquely in the WX group, respectively (Table S9 and S10). A total of 3551 genes were induced across all 24 tissues, and 37 genes were induced in >7 tissues (Fig. 4B, C).

Previously-reported p53-target genes, Eda2r (Tanikawa et al., 2009), Cdkn1a, Trp53inp1, Gdf15, Ccng1, and Aen, were induced in >18 tissues (Fig. 4C and S7). We also identified potential p53 target genes, including Mgmt, Ces2e, Ephx1, Sesn2, and Dcxr, which were induced in >16 tissues. We could obtain the expression data of 144 genes among 150 previously-reported p53 targets. We found 80 known targets (55.6%) were induced in at least one tissues, while 64 genes (44.4%) were not significantly induced in any of the 24 tissues we examined (Table S11 and Fig. S7), indicating a remarkable diversity in the p53-mediated DNA damage response across species and tissue types. In addition, 2576 genes were repressed across the 24 tissues (Fig. 4B).

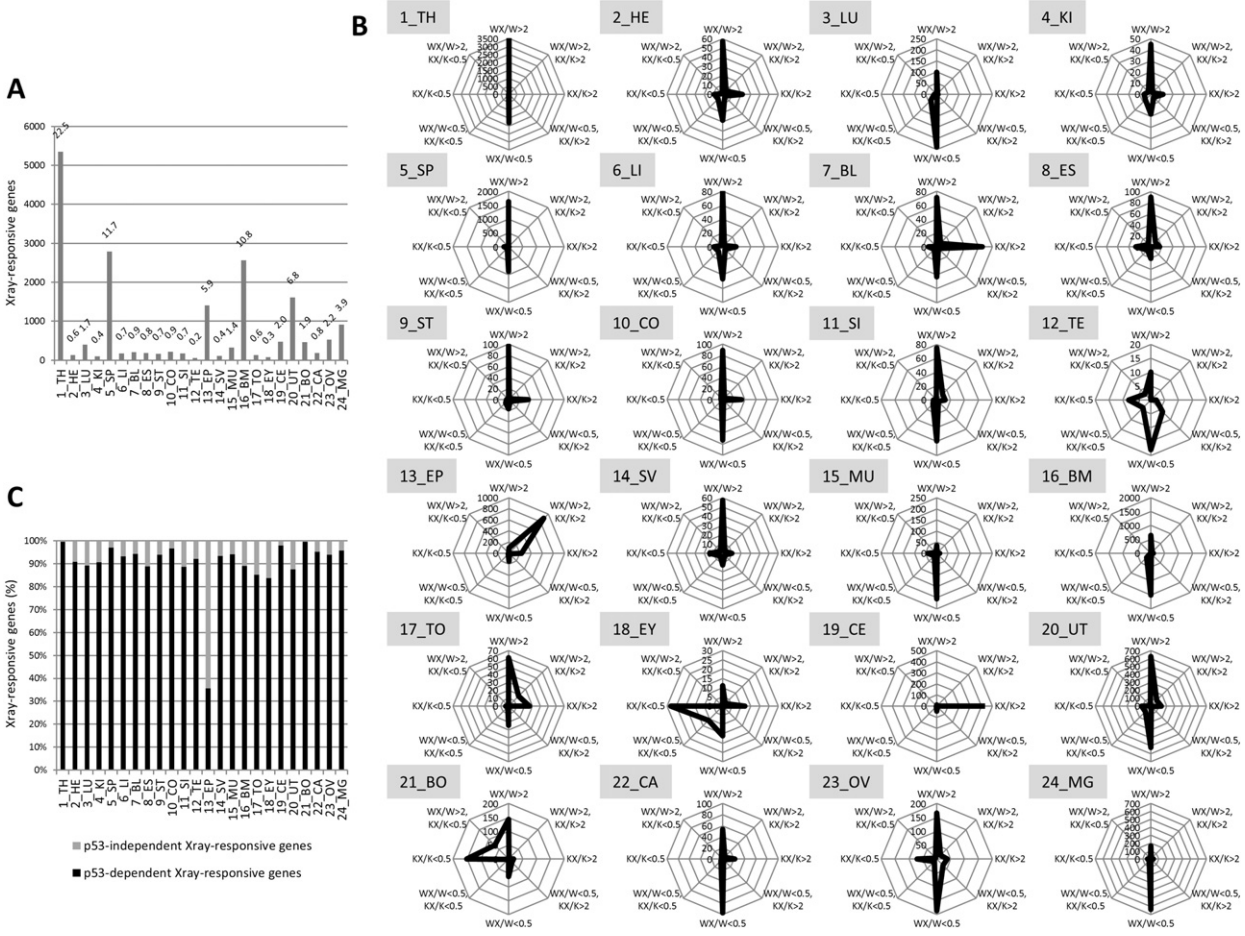

Fig. 2. The regulation of gene expression by p53 in response to X-ray. A, The number of genes whose expression was induced or repressed by more than twofold after X-ray irradiation in $p53^{-/-}$ or $p53^{+/+}$ mice. We added 1 to each FPKM value to filter out genes with low expression levels in this analysis. B, Based on relative changes after X-ray irradiation in wild-type or knockout mice, each gene was categorized into nine groups. Genes that were not induced or reduced more than twofold by X-ray in both $p53^{-/-}$ or $p53^{+/+}$ mice were defined as X-ray non-responsive genes. The number of genes in eight groups except X-ray non-responsive genes was shown by Radar plots. The horizontal and vertical axes indicate the number of genes which show more than twofold change in knockout mice ((KX + 1)/(K + 1)) and wild type mice ((WK + 1)/(W + 1)), respectively. C, The fraction of p53-dependent X-ray-responsive genes among the X-ray-responsive genes in each tissue. When the induction/repression pattern was not identical between $p53^{+/+}$ and $p53^{-/-}$ mice, we defined those as p53-dependent X-ray responsive genes.

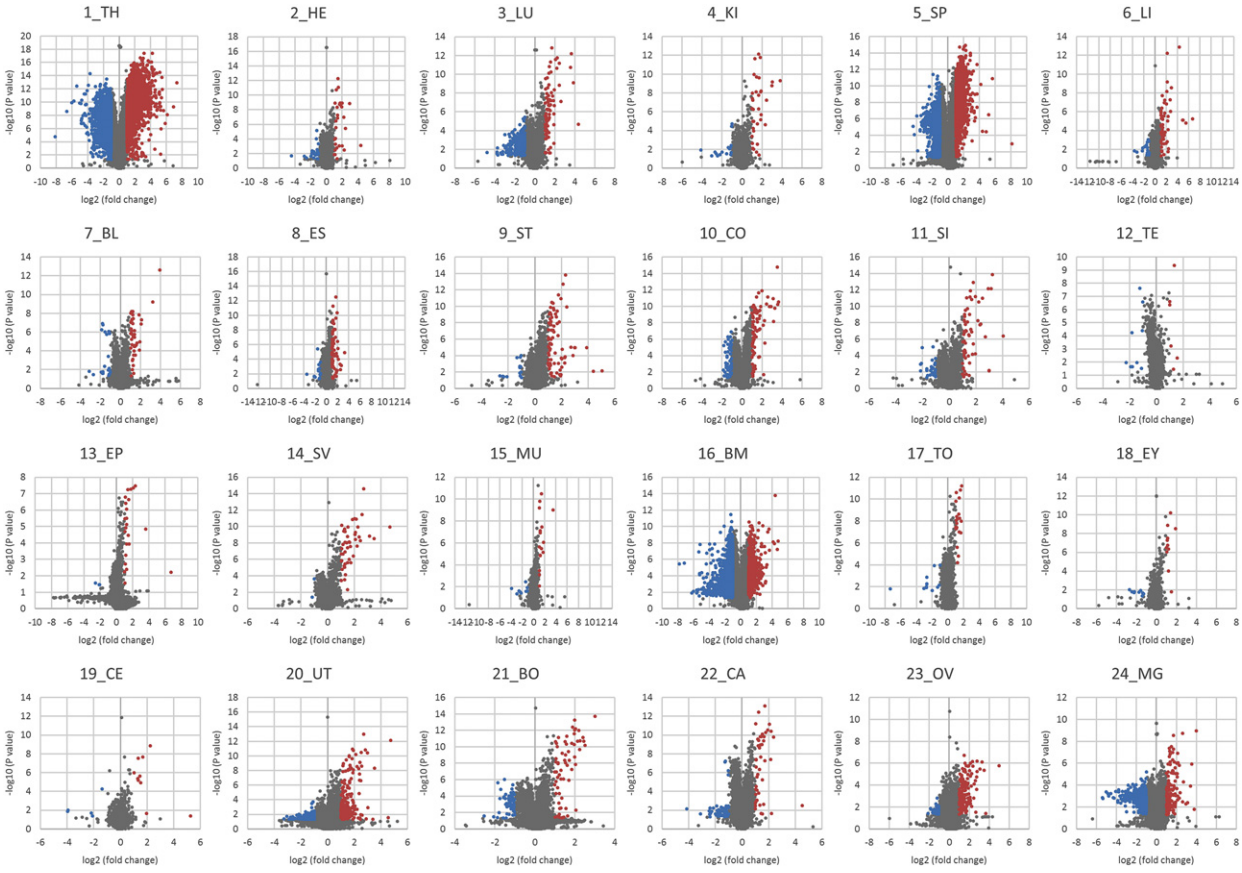

Fig. 3. The transcriptional landscape after p53 activation. The volcano plots showed the gene expression fold change in WX mice compared with other groups (x axis) and its significance (y axis), with each dot representing an individual gene. Significantly induced or repressed genes showing more than twofold change are coloured in red or blue, respectively ($P < 0.05$ by Student's *t*-test).

Then we analyzed published CHIP-seq and RNA-seq data of mouse embryonic fibroblast (MEF) treated with Adriamycin for 6 h (Kenzelmann Broz et al., 2013). CHIP-seq data indicated that p53 could bind 20.87% of p53-induced (741 genes among 3551 genes) and 14.36% of p53-repressed (370 genes among 2576 genes) genes (Table S9 and Fig. S8A, B). In addition, 8.50% of p53-induced (302 genes among 3551 genes) and 3.53% of p53-repressed (91 genes among 2576 genes) genes were also induced and repressed in MEF by Adriamycin treatment. Although different types of cells and DNA damage were used for CHIP-seq and RNA-seq analysis, these set of genes are likely to be direct p53 targets.

3.4. Pathways Modifying p53 Mediated DNA Damage Response

In response to DNA damage, p53 is phosphorylated and activated through ATM-CHK2 pathway (Fei and El-Deiry, 2003). Interestingly, the numbers of p53-induced and p53-repressed genes associates with basal (W) *p53* mRNA expression levels in individual tissues with the correlation coefficient of 0.7172 and 0.6357, respectively (Fig. 4D). Atm and Chek2 expression is also associated with the numbers of p53-induced and p53-repressed genes (Fig. S9). These data clearly indicate the regulation of DNA damage response by Atm-Chk2-p53 cascade. In addition to these genes, 353 and 357 genes exhibit strong association with the number of p53-induced and p53-repressed genes (R2 > 0.6), respectively (Table S12). GO analysis indicated that genes related with transcriptional regulation were enriched (Table S13), suggesting their function as a p53-coactivator. These sets of genes were likely to regulate p53-mediated DNA damage response.

We also analyzed the association of *Cdkn1a* fold activation with basal expression (W) of *p53*, *Atm*, and *Chek2*, in each tissue. *Cdkn1a* fold activation was associated with basal Atm, p53, and Chek2 level ($R^2 = 0.551$, 0.398, and 0.193, respectively, Fig. S10A). Moreover, we found 258 genes that showed strong correlation (R2 > 0.5) with *Cdkn1a* fold activation (Table S14). Pathway analysis of these 258 genes indicated that Jak-STAT pathway and NF-kappa B pathway exhibit significant association with *P*-value of 7×10^{-9} and 6×10^{-7}, respectively (Table S15 and Fig. S10B). Cdkn1a expression was shown to be regulated by multiple pathways including JAK1/STAT1 and TNF (Bhunia et al., 2002; Chin et al., 1996), indicating the feasibility of this analysis to identify modifier of Cdkn1a transactivation.

3.5. Pathway Regulated by p53

We then analyzed the characteristics of p53-regulated genes. Pathway analysis of p53-induced genes in each tissues revealed that "cytokine-cytokine receptor interaction" was significantly associated in five tissues, while "antigen processing and presentation" was associated with p53-repressed genes in eight tissues (Fig. 5 and Table S16). We also visualized the non-redundant GO term set of 3551 p53-induced or 2576 p53-repressed genes (Fig. S11). p53-induced genes were related to diverse functions, such as "response to wounding", "immune response", and "cell adhesion". Moreover, p53-repressed genes were associated with "DNA metabolism", "cell cycle", and "immune system development".

3.6. p53 Signalling Pathway and Human Carcinogenesis

To investigate the role of p53 downstream genes in human carcinogenesis, we analyzed the association of p53-regulated genes with p53 mutations in its corresponding cancer tissues using TCGA (The cancer

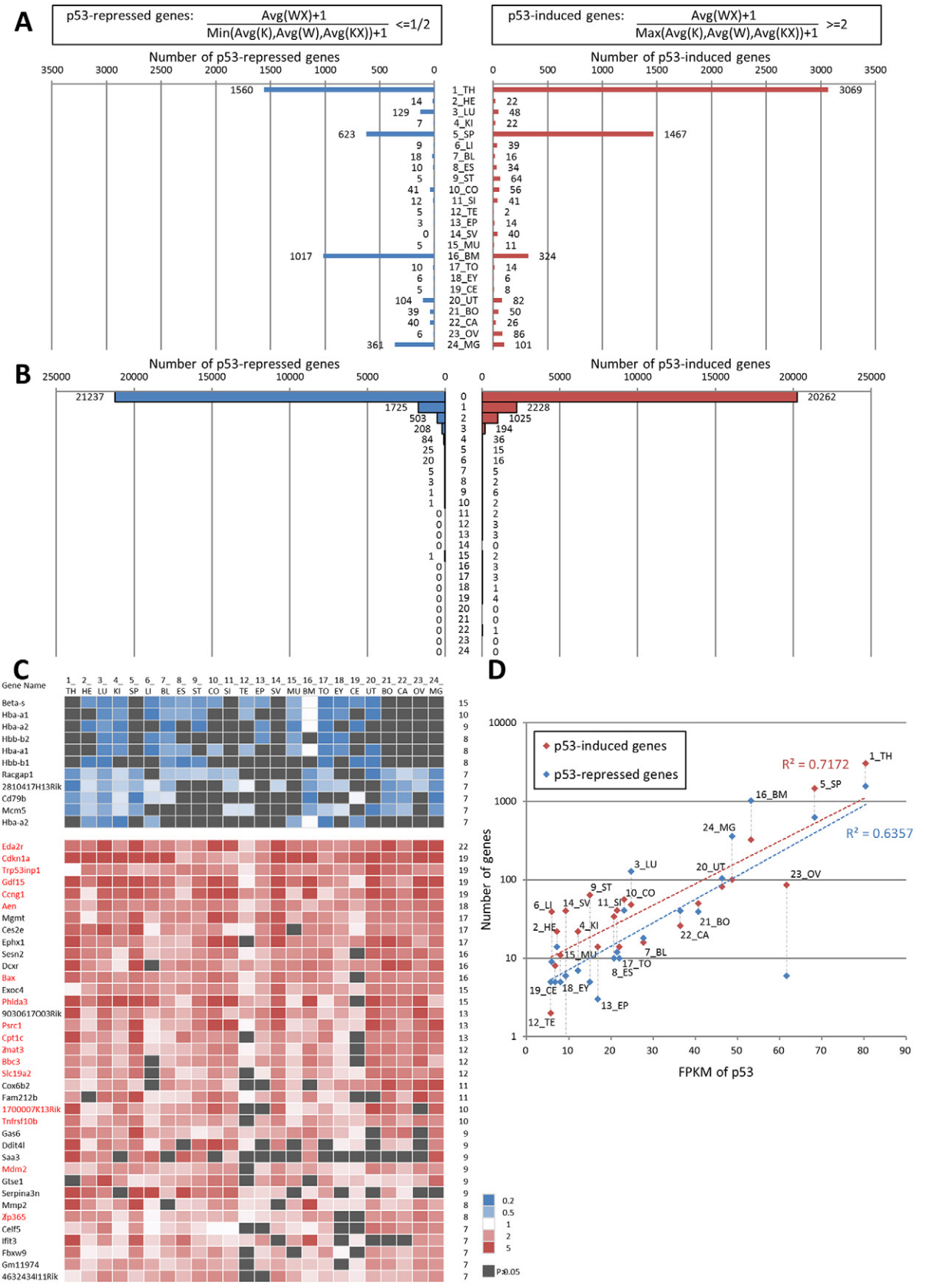

Fig. 4. Screening of p53 targets. A, The number of p53-repressed (left) or p53-induced (right) genes in each tissue was shown. We selected genes that met the following criteria: 1) formula shown in above; 2) WX was significantly different from the remaining samples (W, K, and KX; $P < 0.05$ by Student's *t*-test). B, Genes were categorized based on the number of tissues repressed (left) or induced (right) by p53. C, A list of 11 and 37 genes that were repressed or induced in >7 tissues. Each colour represents the fold change calculated using the formula shown in Fig. 4A. The right column shows the number of tissues. D, The correlation of *p53* expression with the number of p53-induced (red) or p53-repressed genes (blue) in each tissue. X-axis indicates average FPKM value of *p53* gene in $p53^{+/+}$ mice without X-ray (W, n = 2 or 3). Y-axis is the number of p53-induced and p53-repressed genes.

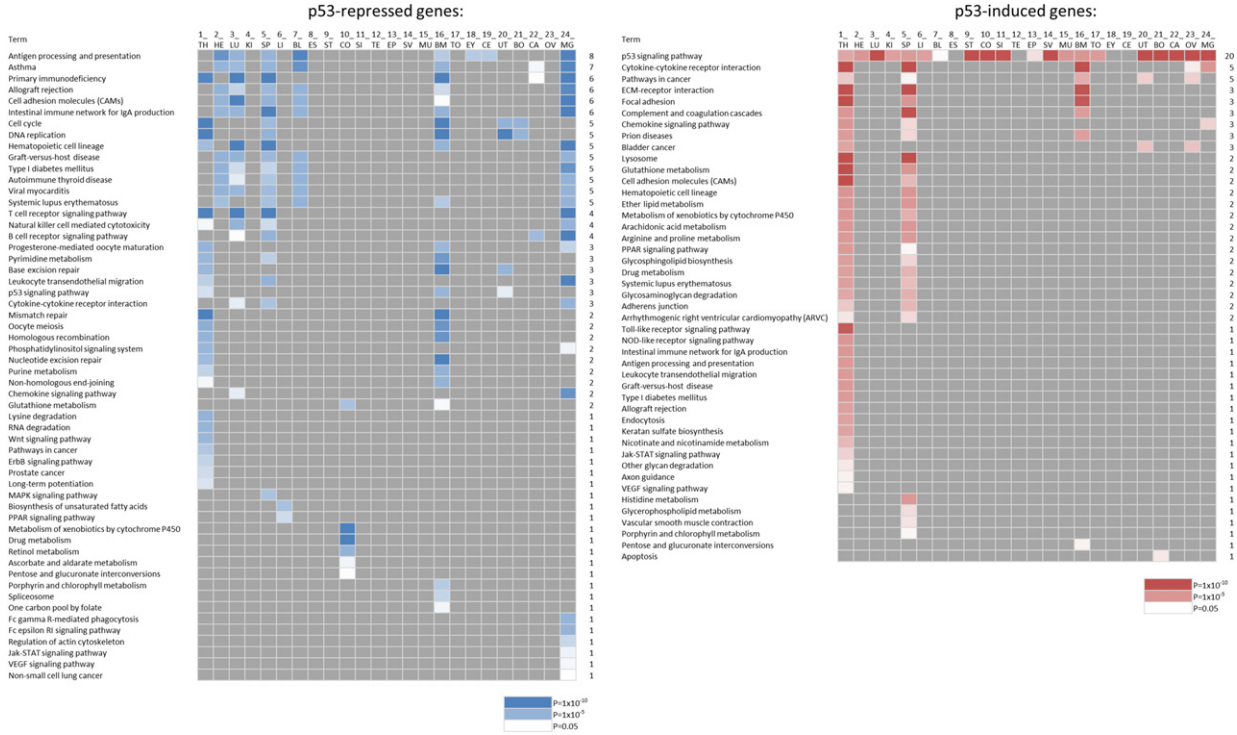

Fig. 5. Pathway analysis of p53 targets. A pathway analysis of p53-repressed (left) or p53-induced (right) genes in each tissue. Each colour represents the *P*-value as shown below. The right column shows the number of tissues.

genome atlas) database (Cancer Genome Atlas, 2012a, 2012b; Cancer Genome Atlas Research, 2011, 2014a) including >5000 cancer tissues of 11 tumor types (Table S17). Around 20% of p53-induced genes were significantly decreased in cancer tissues with p53 mutation (Fig. 6A and Table S18). In addition, nearly half of p53-repressed genes in mammary gland or uterus exhibited higher expression in breast or uterus cancer tissues with p53 mutations. Among these genes regulated by p53 in both human and mouse tissues, we selected 12 genes those were related with key carcinogenic pathway or molecular target therapies (Cheng et al., 2015) (Fig. 6B). Interestingly, four previously reported p53 targets (*CDKN1*, *MDM2*, *BBC3*, and *PLK2*) showed increased expression in various cancer tissues with wild-type p53 compared with those with mutant p53, while eight p53-repressed genes (*AURKB*, *BTK*, *CTLA4*, *ICOSLG*, *IKZF1*, *PIK3CD*, *SH2D1A*, *and SYK*) in mouse mammary gland were repressed in breast cancer tissues with wild-type p53. Because these p53-repressed genes encode therapeutic targets or pathways of cancer (Burger, 2014; Hole et al., 2015; Snyder et al., 2014), combination of therapeutics targeting these molecules might be applicable for triple negative breast cancers in which p53 mutations are frequently observed (Shah et al., 2012). Our whole body transcriptome analysis revealed the molecular pathways regulated by p53 and its possible application in cancer therapeutics.

3.7. Regulation of RNA Splicing by p53

We further explored RNA sequence data at isoform level for all 24 tissues. As a result, we identified another 214 p53-induced genes and 296 p53-repressed genes that we could not identify by gene level analyses (Table S19 and S20). We found remarkable difference in DNA damage response between isoforms. For example, Fbxw7 and Jak2 expression was not affected by p53 at gene level. However, isoforms NM_080428 (Fbxw7, transcript variant 3) and NM_001048177 (Jak2, transcript variant 2) were remarkably induced by p53, while isoforms NM_001177774 (Fbxw7, transcript variant 1), NM_001177773 (Fbxw7, transcript variant 2), and NM_008413 (Jak2, transcript variant 1) were repressed (Fig. S12). Fbxw7 variant 1 and 2 encode the same protein, but Fbxw7 variant 3 has an alternate 5′ exon including coding region and encodes shorter protein with different N-terminus compared to variant 1 and 2. Concordant with our findings, difference in stress response among FBXW7 isoforms was previously reported in human colorectal cancer cells (Sionov et al., 2013). Taken together, our results elucidate the role of p53 in the regulation of alternative splicing.

In addition, p53 induced various p63 isoforms including DNp63beta (NM_001127262) and DNp63 isoform e (NM_001127264) in response to X-ray in thymus (Fig. S12). DNp63 isoforms lack the transactivation domain and function as inhibitors of p53 and TAp63 proteins (Ghioni et al., 2002; Yang et al., 1998). These isoform level analyses suggested p53-DNp63 negative feedback pathway in thymus tissue.

3.8. Regulation of Keratinization in Stomach by p53

Next we focused on p53-induced genes whose expressions were restricted in specific tissues. Among 8117 genes that are highly expressed (>10 FPKM) in up to five tissues, p53 induced expression of 237 genes (Fig. 7A and Table S10 and S21). Interestingly, only the *Cpt1c* gene was previously reported as a p53-target gene, indicating the feasibility of our screening method to identify tissue-specific p53 targets.

Among them, three keratin family members (Krt6a, Krt6b, and Krt17) were induced in stomach (Table S21). In addition, GO analysis of 64 p53-induced genes in stomach revealed that p53 regulates keratinization ($P = 8.24 \times 10^{-10}$, Table S22). Among 52 Keratin family members, 6 keratins (Krt5, Krt6a, Krt6b, Krt14, Krt16, and Krt17) were induced by X-ray in stomach of *p53* $^{+/+}$ mice (Fig. 7B and S13A). qPCR analysis indicated that these keratin family members were induced under various conditions by X-ray irradiation only in *p53*$^{+/+}$ mice (Fig. S13B). Keratin family members cluster on mouse chromosome 15F2 and 11D (Fig. S14A). We surveyed the consensus p53-binding sequence (p53BS) within these loci and found 30 potential p53BSs (Table S3). We conducted a reporter assay and found 7 p53BSs on Chr. 15F2 and 5 p53BSs on Chr. 11D that exhibited a more than five-fold induction in reporter gene activity after co-transfection of wild-type p53

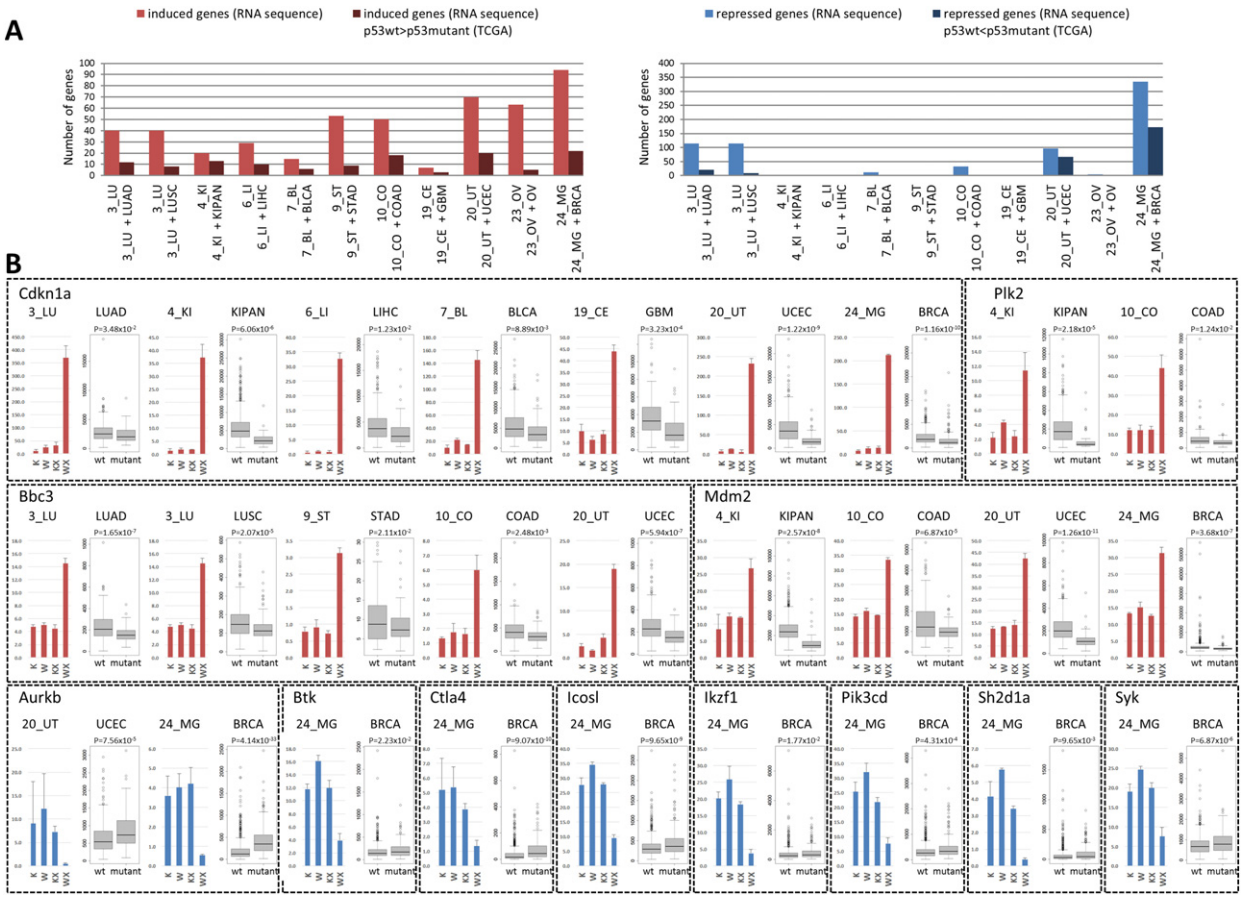

Fig. 6. The p53 signalling pathway and human carcinogenesis. A, The association of p53 regulation in mouse tissue with the expression in their corresponding cancer tissues with or without p53 mutation. We used the RNA sequence data and whole exon sequence data of 11 cancer types from the TCGA database for this analysis. The number of p53-regulated genes in mouse tissue is shown in light blue (p53-repressed genes) or light red (p53-induced genes). The number of genes whose expression is significantly associated with p53 mutation status of cancer tissues is shown in dark blue (p53-repressed genes) or dark red (p53-induced genes). B, p53-regulated genes those are related with key carcinogenic pathway or molecular target therapies (344 genes analyzed in MSK-IMPACT). Expression of four p53-induced (upper and middle) or eight p53-repressed (lower) genes those are significantly associated with p53 mutation status in the corresponding human cancer tissues ($P < 0.05$). (Left) The *y*-axis indicates the FPKM values in each group (K, KX, W, and WX) with S.D. (Right) Gene expression in human cancer tissues. wt; cancer tissues without p53 mutation. Mutant; cancer tissues with a p53 mutation. The vertical axis indicates the normalized expression level, the top bar represents a maximum observation, the lower bar represents a minimum observation, the top of the box is upper or third quartile, the bottom of the box is lower or first quartile, and the middle bar is the median. The association between wt and mutant was assessed using a Student's *t*-test.

(Fig. S14B). Moreover, previous CHIP-seq data using mouse embryonic fibroblast (Kenzelmann Broz et al., 2013) indicated the binding of p53 protein to *Krt5* locus (Ch15: 101545689 $P = 7.34 \times 10^{-23}$, and Ch15: 101547208 $P = 4.76 \times 10^{-22}$ within 30 bp of Ch15F2_3 and Ch15F2_4, respectively, Fig. S14A), suggesting the direct regulation of keratins by p53.

Immunohistochemical analysis showed the induction of Krt6, Krt16, and loricrin, a marker of terminal epidermal differentiation, in forestomach of $p53^{+/+}$ mice by X-ray irradiation (Fig. 7C and S15). Krt6 and loricrin were also induced in glandular stomach of $p53^{+/+}$ mice. On the other hand, the proliferation marker, Ki-67 was decreased in both forestomach and glandular stomach (Fig. S15). We also confirm the induction of Krt6, 16, 17, and p53 protein by X-ray in forestomach of $p53^{+/+}$ mice by western blotting (n = 3 per group, Fig. 7D). These findings demonstrated the regulation of keratinization and differentiation of epithelial cells in stomach by p53 in response to DNA damage.

4. Discussion

The regulation of gene expression by p53 has been extensively analyzed (Idogawa et al., 2014; Kenzelmann Broz et al., 2013), however most of the previous studies analyzed one or two human/mouse cells or tissues as shown in Table S1. Since *p53* mutations were observed in cancers from multiple tissues, the identification of p53-regulated genes in various cell types is essential to fully understand the p53 signalling network. Here, we conducted an RNA sequence-based whole-body transcriptome analysis using $p53^{+/+}$ and $p53^{-/-}$ mice. In our study, 280 samples from 24 tissues were analyzed, andB transcriptome analysis of p53 regulated genes. Our results also indicated that the great majority of X-ray-responsive genes were regulated by p53 and further supported the crucial roles of p53 in the DNA damage response.

In the previous analysis, cells or mice were treated with various dose of radiation (1–10 Gy) and were analyzed at various time points (1–24 h) (Table S1). p53 was induced at 3–6 h after irradiation in thymus, spleen and small intestine, however sensitivity to irradiation varies between tissues (Fei et al., 2002; Komarova et al., 2000). p53 deficient mice exhibited apoptosis resistance and prolonged survival after 10 Gy of radiation (Komarova et al., 2004), suggesting that p53 targets related with apoptotic pathway were induced in this condition. Genes related with apoptotic pathway were shown to be induced relatively late time point in response to severe DNA damage (Oda et al., 2000). Thus, we selected 10 Gy and 24 h in our study to identify p53 targets even in radiation resistant tissues.

We also found remarkable differences in the DNA damage response across different tissues. >2000 genes were regulated in the thymus and spleen in $p53^{+/+}$ mice. These two tissues are known to be sensitive to radiation-induced apoptosis (Gottlieb et al., 1997; Midgley et al., 1995) and commonly develop cancer in p53-defective

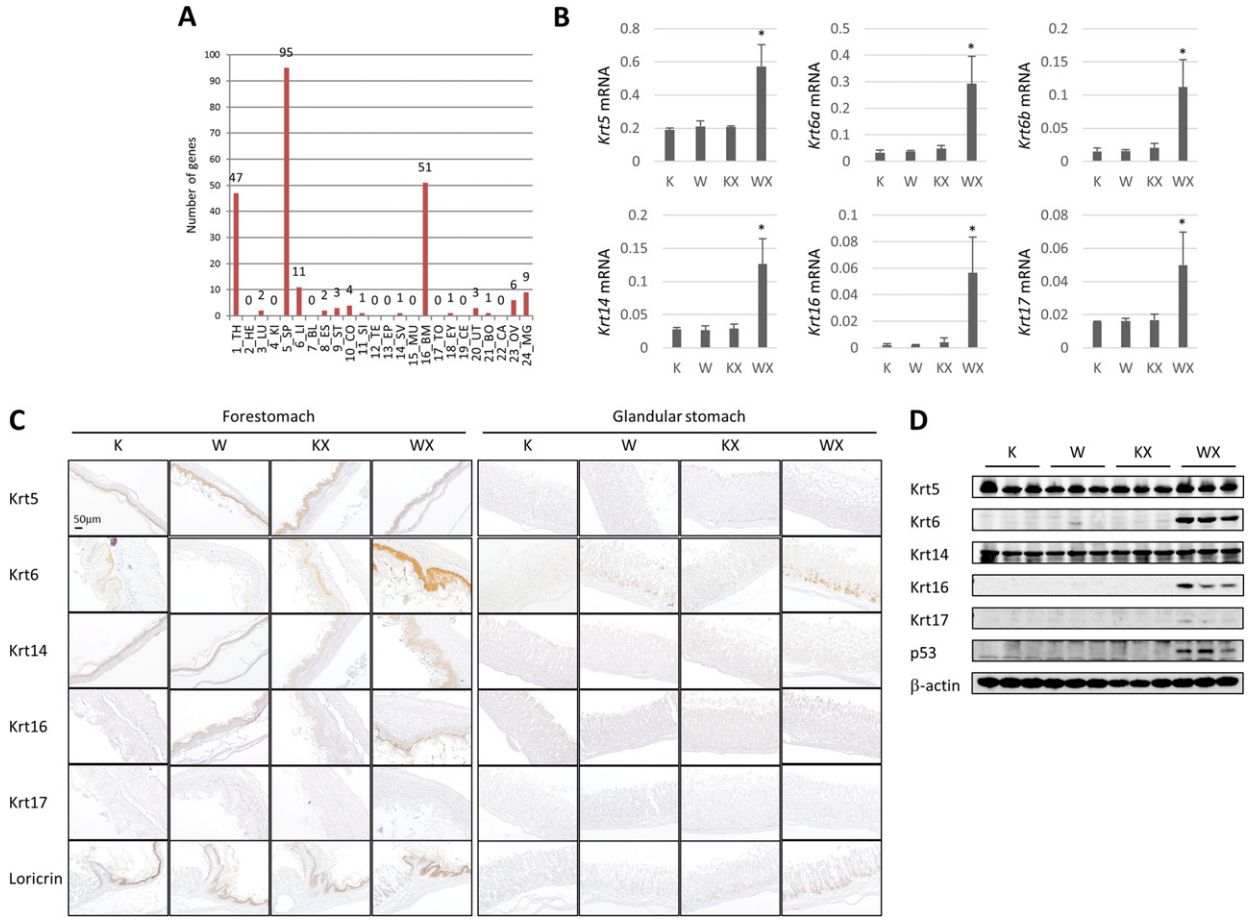

Fig. 7. Tissue-specific targets of p53. A, The number of genes expressed in a limited number of tissues (>10 FPKM in 1 to 5 tissues) and induced by p53 in each tissue. B, qPCR analysis of keratins in the stomach after X-ray irradiation. Mice stomachs were collected 24 h after 10 Gy of X-ray irradiation. Expression in WX was significantly increased compared with other groups (K, W, and KX) (*$P < 0.05$ by Student's *t*-test) (n = 3 per group). C, Immunohistochemical analysis of keratins and loricrin in the forestomach and glandular stomach 48 h after irradiation. K and W indicate $p53^{-/-}$ and $p53^{+/+}$ mice, respectively. X indicates treatment with 20 Gy of X-ray irradiation. D, western blotting of keratins, loricrin, and p53 in the glandular stomach 48 h after irradiation. β-actin was used as a loading control. K and W indicate $p53^{-/-}$ and $p53^{+/+}$ mice, respectively. X indicates treatment with 20 Gy of X-ray irradiation.

mice (Donehower et al., 1995). Expression of p53, Atm, and Chek2 was strongly correlated with the number of p53-regulated genes as well as fold induction of Cdkn1a. Taken together, we revealed that Atm-Chek2-p53 axis was associated with DNA damage response and cancer susceptibility. However, p53 protein was increased in only nine tissues among 22 tissues analyzed. Interesting, both X-ray sensitive (thymus and spleen) and X-ray resistant tissues (testis and heart) exhibited high basal p53 expression with no or marginal p53 induction by X-ray. These results indicate that p53 protein expression cannot fully explain difference in DNA damage response among tissues. Further analyses of genes or pathways that are associated with the number of p53-resposive genes as well as p53 modification are necessary to understand the molecular mechanism of p53-mediated transcriptional regulation.

p53 was shown to repress gene expression by several indirect mechanisms such as p21-DREAM-CDE/CDR pathway (Fischer et al., 2016) or miRNA-mediated pathway (Hermeking, 2012). We found that p53 can bind to a relatively small subset of p53-repressed genes (14.36%) compared with p53-induece genes (20.87%). Our findings also suggest that most of p53-repressed genes are regulated by indirect mechanisms.

Annotation using TCGA database revealed that p53-repressed targets in mouse mammary gland such as *BTK*, *AURKB*, *SYK*, *PIK3CD*, and *CTLA4* are significantly transactivated in human breast cancer tissues with p53 mutations. AURKB, BTK, ICOSLG, SYK, and PIK3CD (Eifert et al., 2013; Katz et al., 2010; Ou et al., 2014; Sawyer et al., 2003) are associated with proliferation or poor prognosis of breast cancers, while CTLA4 is essential for the function of regulatory T cells which suppress cytotoxic T-cell (Vignali et al., 2008). Therefore, p53 would inhibit tumorigenesis by suppressing cell growth and enhancing immune response. Thus, combination of therapeutics targeting these molecules (Friedberg et al., 2010) would be applicable for breast cancers with p53 mutation that are associated with poor prognosis (Bergh et al., 1995).

Our analysis also identified pathways that are regulated by p53 in a tissue-specific manner. Six keratin family members (krt5-krt14, krt6-krt16, and krt6-krt17) induced by p53 are components of intermediate filament. These keratins are induced by skin injury and promote would healing (DePianto and Coulombe, 2004). Mutations of KRT5 and KRT14 result in fragile epidermides and hereditary epidermolysis bullosa simplex (Bonifas et al., 1991), while both $krt5^{-/-}$ (Peters et al., 2001) and $krt14^{-/-}$ (Vassar et al., 1991) mice die soon after birth due to blister formation, which is partially rescued by overexpression of krt16 (Paladini and Coulombe, 1999). In addition, krt6a and krt6b double knockout mice showed increased ulceration in upper digestive tract (Wong et al., 2000), indicating their important roles in the maintenance of epithelial integrity. Thus, p53 would protect gastric mucosa from radiation-induced injury by inducing keratin family members.

Taken together, our comprehensive analysis of p53 target genes revealed the crucial role of p53 as a master regulator of the DNA damage response in most of tissues. Because the mutation of *p53* is the most common genetic alteration in cancer tissues, our results would elucidate

tissue specific roles of p53 that will enhance our understanding of cancer biology.

Supplementary data to this article can be found online at http://dx.doi.org/10.1016/j.ebiom.2017.05.017.

Funding Sources

This work was supported by Ministry of Education, Culture, Sports, Science and Technology of Japan [25134707 and 16H01566 to K.M., 15K14377 to C.T.].

Conflict of Interest

The authors declare no conflict of interest.

Author Contributions

C.T. conducted all the experiments and analyzed the data. Y.Z.Z., S.I., R.Y., S.M, and H.N. contributed to the analyses of RNA-seq data. Y.T., M.T., Y.F., and J.I assisted sample preparation. R.Y. conducted the analysis of stomach tissues. C.T., Y.N., and K.M.

Acknowledgement

We thank Takashi Fujitomo, Paulisally Hau Yi Lo, Tomoyuki Kogushi, Satoyo Oda, and Satomi Takahash for technical assistance.

References

Bergh, J., Norberg, T., Sjogren, S., Lindgren, A., Holmberg, L., 1995. Complete sequencing of the p53 gene provides prognostic information in breast cancer patients, particularly in relation to adjuvant systemic therapy and radiotherapy. Nat. Med. 1, 1029–1034.

Bhunia, A.K., Piontek, K., Boletta, A., Liu, L., Qian, F., Xu, P.N., Germino, F.J., Germino, G.G., 2002. PKD1 induces p21(waf1) and regulation of the cell cycle via direct activation of the JAK-STAT signaling pathway in a process requiring PKD2. Cell 109, 157–168.

Bonifas, J.M., Rothman, A.L., Epstein Jr., E.H., 1991. Epidermolysis bullosa simplex: evidence in two families for keratin gene abnormalities. Science 254, 1202–1205.

Brooks, M.J., Rajasimha, H.K., Roger, J.E., Swaroop, A., 2011. Next-generation sequencing facilitates quantitative analysis of wild-type and Nrl(−/−) retinal transcriptomes. Mol. Vis. 17, 3034–3054.

Burger, J.A., 2014. Bruton's tyrosine kinase (BTK) inhibitors in clinical trials. Curr. Hematol. Malig. Rep. 9, 44–49.

Cancer Genome Atlas, N, 2012a. Comprehensive molecular characterization of human colon and rectal cancer. Nature 487, 330–337.

Cancer Genome Atlas, N, 2012b. Comprehensive molecular portraits of human breast tumours. Nature 490, 61–70.

Cancer Genome Atlas Research, N, 2011. Integrated genomic analyses of ovarian carcinoma. Nature 474, 609–615.

Cancer Genome Atlas Research, N, 2013. Comprehensive molecular characterization of clear cell renal cell carcinoma. Nature 499, 43–49.

Cancer Genome Atlas Research, N, 2014a. Comprehensive molecular profiling of lung adenocarcinoma. Nature 511, 543–550.

Cancer Genome Atlas Research, N, 2014b. Integrated genomic characterization of papillary thyroid carcinoma. Cell 159, 676–690.

Cao, L., Li, W., Kim, S., Brodie, S.G., Deng, C.X., 2003. Senescence, aging, and malignant transformation mediated by p53 in mice lacking the Brca1 full-length isoform. Genes Dev. 17, 201–213.

Chen, X., Bahrami, A., Pappo, A., Easton, J., Dalton, J., Hedlund, E., Ellison, D., Shurtleff, S., Wu, G., Wei, L., et al., 2014. Recurrent somatic structural variations contribute to tumorigenesis in pediatric osteosarcoma. Cell Rep. 7, 104–112.

Cheng, D.T., Mitchell, T.N., Zehir, A., Shah, R.H., Benayed, R., Syed, A., Chandramohan, R., Liu, Z.Y., Won, H.H., Scott, S.N., et al., 2015. Memorial Sloan Kettering-integrated mutation profiling of actionable cancer targets (MSK-IMPACT): a hybridization capture-based next-generation sequencing clinical assay for solid tumor molecular oncology. J. Mol. Diagn. 17, 251–264.

Chin, Y.E., Kitagawa, M., Su, W.C., You, Z.H., Iwamoto, Y., Fu, X.Y., 1996. Cell growth arrest and induction of cyclin-dependent kinase inhibitor p21 WAF1/CIP1 mediated by STAT1. Science 272, 719–722.

DePianto, D., Coulombe, P.A., 2004. Intermediate filaments and tissue repair. Exp. Cell Res. 301, 68–76.

Donehower, L.A., Harvey, M., Slagle, B.L., McArthur, M.J., Montgomery Jr., C.A., Butel, J.S., Bradley, A., 1992. Mice deficient for p53 are developmentally normal but susceptible to spontaneous tumours. Nature 356, 215–221.

Donehower, L.A., Harvey, M., Vogel, H., McArthur, M.J., Montgomery Jr., C.A., Park, S.H., Thompson, T., Ford, R.J., Bradley, A., 1995. Effects of genetic background on tumorigenesis in p53-deficient mice. Mol. Carcinog. 14, 16–22.

Dulak, A.M., Stojanov, P., Peng, S., Lawrence, M.S., Fox, C., Stewart, C., Bandla, S., Imamura, Y., Schumacher, S.E., Shefler, E., et al., 2013. Exome and whole-genome sequencing of esophageal adenocarcinoma identifies recurrent driver events and mutational complexity. Nat. Genet. 45, 478–486.

Eifert, C., Wang, X., Kokabee, L., Kourtidis, A., Jain, R., Gerdes, M.J., Conklin, D.S., 2013. A novel isoform of the B cell tyrosine kinase BTK protects breast cancer cells from apoptosis. Genes Chromosom. Cancer 52, 961–975.

Fei, P., El-Deiry, W.S., 2003. P53 and radiation responses. Oncogene 22, 5774–5783.

Fei, P., Bernhard, E.J., El-Deiry, W.S., 2002. Tissue-specific induction of p53 targets in vivo. Cancer Res. 62, 7316–7327.

Fischer, M., Quaas, M., Steiner, L., Engeland, K., 2016. The p53-p21-DREAM-CDE/CHR pathway regulates G2/M cell cycle genes. Nucleic Acids Res. 44, 164–174.

Friedberg, J.W., Sharman, J., Sweetenham, J., Johnston, P.B., Vose, J.M., LaCasce, A., Schaefer-Cutillo, J., De Vos, S., Sinha, R., Leonard, J.P., 2010. Inhibition of Syk with fostamatinib disodium has significant clinical activity in non-Hodgkin lymphoma and chronic lymphocytic leukemia. Blood 115, 2578–2585.

Ghioni, P., Bolognese, F., Duijf, P.H., Van Bokhoven, H., Mantovani, R., Guerrini, L., 2002. Complex transcriptional effects of p63 isoforms: identification of novel activation and repression domains. Mol. Cell. Biol. 22, 8659–8668.

Gottlieb, E., Haffner, R., King, A., Asher, G., Gruss, P., Lonai, P., Oren, M., 1997. Transgenic mouse model for studying the transcriptional activity of the p53 protein: age- and tissue-dependent changes in radiation-induced activation during embryogenesis. EMBO J. 16, 1381–1390.

Hermeking, H., 2012. MicroRNAs in the p53 network: micromanagement of tumour suppression. Nat. Rev. Cancer 12, 613–626.

Hingorani, S.R., Wang, L., Multani, A.S., Combs, C., Deramaudt, T.B., Hruban, R.H., Rustgi, A.K., Chang, S., Tuveson, D.A., 2005. Trp53R172H and KrasG12D cooperate to promote chromosomal instability and widely metastatic pancreatic ductal adenocarcinoma in mice. Cancer Cell 7, 469–483.

Hole, S., Pedersen, A.M., Lykkesfeldt, A.E., Yde, C.W., 2015. Aurora kinase A and B as new treatment targets in aromatase inhibitor-resistant breast cancer cells. Breast Cancer Res. Treat. 149, 715–726.

Hu, W., Feng, Z., Teresky, A.K., Levine, A.J., 2007. p53 regulates maternal reproduction through LIF. Nature 450, 721–724.

Idogawa, M., Ohashi, T., Sasaki, Y., Maruyama, R., Kashima, L., Suzuki, H., Tokino, T., 2014. Identification and analysis of large intergenic non-coding RNAs regulated by p53 family members through a genome-wide analysis of p53-binding sites. Hum. Mol. Genet. 23, 2847–2857.

Jacks, T., Remington, L., Williams, B.O., Schmitt, E.M., Halachmi, S., Bronson, R.T., Weinberg, R.A., 1994. Tumor spectrum analysis in p53-mutant mice. Curr. Biol. 4, 1–7.

Kaartokallio, T., Cervera, A., Kyllonen, A., Laivuori, K., Group, F.C.I, 2015. Gene expression profiling of pre-eclamptic placentae by RNA sequencing. Sci. Rep. 5, 14107.

Kang, H.J., Feng, Z., Sun, Y., Atwal, G., Murphy, M.E., Rebbeck, T.R., Rosenwaks, Z., Levine, A.J., Hu, W., 2009. Single-nucleotide polymorphisms in the p53 pathway regulate fertility in humans. Proc. Natl. Acad. Sci. U. S. A. 106, 9761–9766.

Katz, E., Dubois-Marshall, S., Sims, A.H., Faratian, D., Li, J., Smith, E.S., Quinn, J.A., Edward, M., Meehan, R.R., Evans, E.E., et al., 2010. A gene on the HER2 amplicon, C35, is an oncogene in breast cancer whose actions are prevented by inhibition of Syk. Br. J. Cancer 103, 401–410.

Kenzelmann Broz, D., Spano Mello, S., Bieging, K.T., Jiang, D., Dusek, R.L., Brady, C.A., Sidow, A., Attardi, L.D., 2013. Global genomic profiling reveals an extensive p53-regulated autophagy program contributing to key p53 responses. Genes Dev. 27, 1016–1031.

Komarova, E.A., Chernov, M.V., Franks, R., Wang, K., Armin, G., Zelnick, C.R., Chin, D.M., Bacus, S.S., Stark, G.R., Gudkov, A.V., 1997. Transgenic mice with p53-responsive lacZ: p53 activity varies dramatically during normal development and determines radiation and drug sensitivity in vivo. EMBO J. 16, 1391–1400.

Komarova, E.A., Christov, K., Faerman, A.I., Gudkov, A.V., 2000. Different impact of p53 and p21 on the radiation response of mouse tissues. Oncogene 19, 3791–3798.

Komarova, E.A., Kondratov, R.V., Wang, K., Christov, K., Golovkina, T.V., Goldblum, J.R., Gudkov, A.V., 2004. Dual effect of p53 on radiation sensitivity in vivo: p53 promotes hematopoietic injury, but protects from gastro-intestinal syndrome in mice. Oncogene 23, 3265–3271.

Kruiswijk, F., Labuschagne, C.F., Vousden, K.H., 2015. p53 in survival, death and metabolic health: a lifeguard with a licence to kill. Nat. Rev. Mol. Cell Biol. 16, 393–405.

Liu, X., Holstege, H., van der Gulden, H., Treur-Mulder, M., Zevenhoven, J., Velds, A., Kerkhoven, R.M., van Vliet, M.H., Wessels, L.F., Peterse, J.L., et al., 2007. Somatic loss of BRCA1 and p53 in mice induces mammary tumors with features of human BRCA1-mutated basal-like breast cancer. Proc. Natl. Acad. Sci. U. S. A. 104, 12111–12116.

Lowe, S.W., Schmitt, E.M., Smith, S.W., Osborne, B.A., Jacks, T., 1993. p53 is required for radiation-induced apoptosis in mouse thymocytes. Nature 362, 847–849.

Malkin, D., Li, F.P., Strong, L.C., Fraumeni Jr., J.F., Nelson, C.E., Kim, D.H., Kassel, J., Gryka, M.A., Bischoff, F.Z., Tainsky, M.A., et al., 1990. Germ line p53 mutations in a familial syndrome of breast cancer, sarcomas, and other neoplasms. Science 250, 1233–1238.

Masuda, Y., Futamura, M., Kamino, H., Nakamura, Y., Kitamura, N., Ohnishi, S., Miyamoto, Y., Ichikawa, H., Ohta, T., Ohki, M., et al., 2006. The potential role of DFNA5, a hearing impairment gene, in p53-mediated cellular response to DNA damage. J. Hum. Genet. 51, 652–664.

Midgley, C.A., Owens, B., Briscoe, C.V., Thomas, D.B., Lane, D.P., Hall, P.A., 1995. Coupling between gamma irradiation, p53 induction and the apoptotic response depends upon cell type in vivo. J. Cell Sci. 108 (Pt 5), 1843–1848.

Mori, J., Tanikawa, C., Funauchi, Y., Lo, P.H., Nakamura, Y., Matsuda, K., 2016. Cystatin C as a p53-inducible apoptotic mediator which regulates cathepsin L activity. Cancer Sci. 107, 298–306.

Nakamura, Y., 2004. Isolation of p53-target genes and their functional analysis. Cancer Sci. 95, 7–11.
Oda, K., Arakawa, H., Tanaka, T., Matsuda, K., Tanikawa, C., Mori, T., Nishimori, H., Tamai, K., Tokino, T., Nakamura, Y., et al., 2000. p53AIP1, a potential mediator of p53-dependent apoptosis, and its regulation by Ser-46-phosphorylated p53. Cell 102, 849–862.
Opitz, O.G., Harada, H., Suliman, Y., Rhoades, B., Sharpless, N.E., Kent, R., Kopelovich, L., Nakagawa, H., Rustgi, A.K., 2002. A mouse model of human oral-esophageal cancer. J. Clin. Invest. 110, 761–769.
Ou, O., Huppi, K., Chakka, S., Gehlhaus, K., Dubois, W., Patel, J., Chen, J., Mackiewicz, M., Jones, T.L., Pitt, J.J., et al., 2014. Loss-of-function RNAi screens in breast cancer cells identify AURKB, PLK1, PIK3R1, MAPK12, PRKD2, and PTK6 as sensitizing targets of rapamycin activity. Cancer Lett. 354, 336–347.
Paladini, R.D., Coulombe, P.A., 1999. The functional diversity of epidermal keratins revealed by the partial rescue of the keratin 14 null phenotype by keratin 16. J. Cell Biol. 146, 1185–1201.
Patch, A.M., Christie, E.L., Etemadmoghadam, D., Garsed, D.W., George, J., Fereday, S., Nones, K., Cowin, P., Alsop, K., Bailey, P.J., et al., 2015. Whole-genome characterization of chemoresistant ovarian cancer. Nature 521, 489–494.
Peters, B., Kirfel, J., Bussow, H., Vidal, M., Magin, T.M., 2001. Complete cytolysis and neonatal lethality in keratin 5 knockout mice reveal its fundamental role in skin integrity and in epidermolysis bullosa simplex. Mol. Biol. Cell 12, 1775–1789.
Ramsay, A.J., Martinez-Trillos, A., Jares, P., Rodriguez, D., Kwarciak, A., Quesada, V., 2013. Next-generation sequencing reveals the secrets of the chronic lymphocytic leukemia genome. Clin. Transl. Oncol. 15, 3–8.
Sawyer, C., Sturge, J., Bennett, D.C., O'Hare, M.J., Allen, W.E., Bain, J., Jones, G.E., Vanhaesebroeck, B., 2003. Regulation of breast cancer cell chemotaxis by the phosphoinositide 3-kinase p110delta. Cancer Res. 63, 1667–1675.
Shah, S.P., Roth, A., Goya, R., Oloumi, A., Ha, G., Zhao, Y., Turashvili, G., Ding, J., Tse, K., Haffari, G., et al., 2012. The clonal and mutational evolution spectrum of primary triple-negative breast cancers. Nature 486, 395–399.
Shiraishi, K., Kohno, T., Tanai, C., Goto, Y., Kuchiba, A., Yamamoto, S., Tsuta, K., Nokihara, H., Yamamoto, N., Sekine, I., et al., 2010. Association of DNA repair gene polymorphisms with response to platinum-based doublet chemotherapy in patients with non-small-cell lung cancer. J. Clin. Oncol. 28, 4945–4952.
Sionov, R.V., Netzer, E., Shaulian, E., 2013. Differential regulation of FBXW7 isoforms by various stress stimuli. Cell Cycle 12, 3547–3554.
Snyder, A., Makarov, V., Merghoub, T., Yuan, J., Zaretsky, J.M., Desrichard, A., Walsh, L.A., Postow, M.A., Wong, P., Ho, T.S., et al., 2014. Genetic basis for clinical response to CTLA-4 blockade in melanoma. N. Engl. J. Med. 371, 2189–2199.
Stacey, S.N., Sulem, P., Jonasdottir, A., Masson, G., Gudmundsson, J., Gudbjartsson, D.F., Magnusson, O.T., Gudjonsson, S.A., Sigurgeirsson, B., Thorisdottir, K., et al., 2011. A germline variant in the TP53 polyadenylation signal confers cancer susceptibility. Nat. Genet. 43, 1098–1103.
Tanikawa, C., Furukawa, Y., Yoshida, N., Arakawa, H., Nakamura, Y., Matsuda, K., 2009. XEDAR as a putative colorectal tumor suppressor that mediates p53-regulated anoikis pathway. Oncogene 28, 3081–3092.
Tsukada, T., Tomooka, Y., Takai, S., Ueda, Y., Nishikawa, S., Yagi, T., Tokunaga, T., Takeda, N., Suda, Y., Abe, S., et al., 1993. Enhanced proliferative potential in culture of cells from p53-deficient mice. Oncogene 8, 3313–3322.
Uhlen, M., Fagerberg, L., Hallstrom, B.M., Lindskog, C., Oksvold, P., Mardinoglu, A., Sivertsson, A., Kampf, C., Sjostedt, E., Asplund, A., et al., 2015. Proteomics. Tissue-based map of the human proteome. Science 347, 1260419.
Vassar, R., Coulombe, P.A., Degenstein, L., Albers, K., Fuchs, E., 1991. Mutant keratin expression in transgenic mice causes marked abnormalities resembling a human genetic skin disease. Cell 64, 365–380.
Vignali, D.A., Collison, L.W., Workman, C.J., 2008. How regulatory T cells work. Nat. Rev. Immunol. 8, 523–532.
Vogelstein, B., Lane, D., Levine, A.J., 2000. Surfing the p53 network. Nature 408, 307–310.
Wong, P., Colucci-Guyon, E., Takahashi, K., Gu, C., Babinet, C., Coulombe, P.A., 2000. Introducing a null mutation in the mouse K6alpha and K6beta genes reveals their essential structural role in the oral mucosa. J. Cell Biol. 150, 921–928.
Xue, W., Chen, S., Yin, H., Tammela, T., Papagiannakopoulos, T., Joshi, N.S., Cai, W., Yang, G., Bronson, R., Crowley, D.G., et al., 2014. CRISPR-mediated direct mutation of cancer genes in the mouse liver. Nature 514, 380–384.
Yang, A., Kaghad, M., Wang, Y., Gillett, E., Fleming, M.D., Dotsch, V., Andrews, N.C., Caput, D., McKeon, F., 1998. p63, a p53 homolog at 3q27-29, encodes multiple products with transactivating, death-inducing, and dominant-negative activities. Mol. Cell 2, 305–316.